PHYSICAL REVIEW B VOLUME 40, NUMBER 1 1 JULY 1989

Magnetic and structural properties of amorphous CoTi soft ferromagnetic thin films. I. Magnetic properties

K. Ounadjela, G. Suran, and F. Machizaud
Laboratoire de Magnétisme, Centre National de la Recherche Scientifique, 92195 Meudon CEDEX, France
(Received 18 April 1988; revised manuscript received 30 October 1988)

The magnetic and related structural properties of amorphous $Co_{1-x}Ti_x$ ferromagnetic thin films are reported. The concentration range investigated is $0.14 \le x \le 0.22$. In this first part of the paper the as-obtained magnetic properties are presented. The films were prepared by rf sputtering, and the deposition process was performed in a magnetic field applied parallel to the film surface. The magnetic properties were studied systematically as a function of the pressure of sputtering gas P_{Ar} and rf input power W_{rf}. For the whole concentration range and the overall deposition parameters the ferromagnetic resonance revealed standing spin-wave spectra corresponding to magnetically highly uniform samples. The deposition parameters affect essentially the in-plane uniaxial anisotropy energy K_u and the coercive field H_c along the easy axis. K_u shows a bell-shaped variation as a function of P_{Ar}. The maximum value of K_u $(K_u)_{max}$ is obtained for the same P_{Ar} in the whole concentration range studied. The physical origin of K_u was determined by performing thermomagnetic annealing, which revealed that depending on the value of P_{Ar} used, K_u is related to a pseudodipolar or structural mechanism or a combination of both. The small variations of H_c with deposition parameters are also shown and discussed in terms of the change in the local structure.

I. INTRODUCTION

It is well established that many ferromagnetic alloys respond to field annealing. As a result of the annealing a twofold magnetic anisotropy K_u is induced, the direction of the easy axis of the anisotropy field $H_K = 2K_u/M_s$ being generally parallel to the direction of the applied field.

The dependence of K_u upon the composition, magnetic properties, and conditions of annealing has been widely studied on various soft ferromagnetic crystalline and amorphous materials. Experiments on crystalline alloys have been performed mainly on the FeCoNi system,[1] while investigations on amorphous materials have been concentrated upon various transition-metal (TM)-metalloid (MA) alloys.[2-7] The main results can be summarized as follows: (a) The anisotropy constant K_u is of the same order of magnitude in soft crystalline and soft amorphous TM-MA alloys and is typically in the range of 10^2 to 10^4 erg/cm^3; (b) the magnitude of K_u is much larger both in crystalline and amorphous materials when the alloy is formed of two different magnetic atoms, than in alloys containing only one kind of magnetic element;[4,6,7] and (c) the development and kinetics of orientation of K_u are governed by a reversible relaxation process.[8] In particular, the reorientation of K_u by annealing in a magnetic field along different directions is reversible.

The basic mechanism of the origin of K_u has been attributed to the formation of a directional atomic pair ordering. In alloys containing two different magnetic elements the concentration dependence of K_u could be well explained by the Neel-Taniguchi[9,10] model based upon the diatomic pair ordering mechanism via pseudodipolar interactions. In crystalline alloys with a single type of magnetic atoms, K_u has been related to the ordering of vacancies or interstitials,[11] while in amorphous materials K_u has been attributed to a monoatomic directional order or a pair ordering of a single magnetic species in an inhomogeneous environment.[12]

More recently Co-nonmagnetic-transition-metal (NMT) amorphous alloys were studied by several investigators. The NMT glass-forming element was an early transition metal such as Ti, Zr, Nb, Hf.[13-15] The investigations revealed that these alloys can be obtained with a high saturation magnetization and a small magnetostriction and may have superior soft ferromagnetic properties, and are thus highly promising for various practical applications. Generally these amorphous Co-(NTM) thin films were prepared by sputtering and the various experimenters observed a spontaneous formation of an in-plane uniaxial anisotropy during the preparation process. There exist large discrepancies between the as-reported values of K_u,[13-17] which is probably related to the fact that K_u was studied in thin films where it was formed spontaneously. Consequently, it was not possible to determine the main parameters that define the magnitude of K_u.

In an attempt to understand better the formation and the physical origin of the induced uniaxial anisotropy in this class of material we performed a study on $Co_{1-x}Ti_x$ amorphous thin films. The magnetic and structural properties were studied systematically as a function of concentration and deposition parameters. In order to control the formation of K_u we applied a magnetic field parallel to the film plane during the deposition process.

The present paper is in two independent parts. In this first part we describe the preparation conditions and the magnetic properties of amorphous $Co_{1-x}Ti_x$ thin films. Some of the experimental results and the physical model

 ©1989 The American Physical Society

used to explain the variation of K_u were reported previously,[18–21] and so they will only be recalled briefly. We present new experimental data which enabled us to distinguish experimentally between pseudodipolar and structure-related anisotropy and which also confirm the proposed model. The characterization by ferromagnetic resonance and dependence of the coercive field upon deposition parameters will be given in detail.

The second part of the paper is devoted to the structural investigations. It reports the experimental results studied by electron microscopy, and the structural model is described in detail.

II. EXPERIMENTAL DETAILS

The a-$Co_{1-x}Ti_x$ films were deposited in a conventional rf diode sputtering apparatus, with argon (Ar) as the sputtering gas. Films of composition $x=0.08$ and $x=0.14$ were obtained from vacuum melted targets of composition $Co_{90}Ti_{10}$ and $Co_{86}Ti_{14}$, respectively. The diameters of the targets were 100 and 150 mm, respectively. Films with composition $0.08 \le x \le 0.14$ and $0.14 < x < 0.22$ were obtained, respectively, from the smaller and larger targets by placing radially triangular-shaped 1-mm thick Ti platelets on the vacuum melted targets. The required composition could be obtained by adjusting the number of the Ti platelets. The composition of the films were determined by electron-probe microanalysis. The targets were carefully cooled down by sticking them to the water-cooled cathode. In rf sputtering the main deposition parameters are the background pressure P_b before the introduction of the sputtering gas, the distance between the target and the substrate l, the pressure of the sputter gas P_{Ar}, and the rf input power W_{rf}. The results reported here correspond to $P_b = 10^{-7}$ Torr and $l = 75$ mm. We performed a systematic study of the magnetic and structural properties for 3×10^{-3} Torr $\le P_{Ar} \le 15\times10^{-3}$ Torr and 100 W $\le W_{rf} \le 400$ W, which corresponds to $0.56 W/\mathrm{cm}^2 \le W_{rf}/\mathrm{cm}^2 \le 2.26$ W/cm^2 for the target of 150 mm.

The uniaxial anisotropy K_u was induced by performing the deposition process in a dc magnetic field of 700 Oe applied parallel to the film surface.[22] The schematic configuration of the sample holder, which was fixed on the water-cooled anode, is shown in Fig. 1. It consists of a parallelepiped of copper on which the glass substrates are fixed. On each side of the copper piece we placed a permanent magnet. The permanent magnets were covered by a circular iron plate with a slit in its center through which the deposition took place. The iron plate acts as a magnetic shield. When it covers the permanent magnets the magnetic field is localized outside the plasma. The magnetic field is fairly uniform and parallel to the substrate surface. Visual inspection revealed that the plasma was essentially confined between the target and the iron plate.

This configuration of the sample holder[22] permits the temperature of the substrate surface to be maintained close to room temperature during the deposition process. This effect is simply related to the configuration of the magnetic field which is strictly parallel to the substrate surface, so the main contribution to heating which is the bombardment of the substrate surface by secondary electrons is almost completely suppressed.

This configuration was also necessary in order to avoid the formation of an anisotropy perpendicular to the film plane. When the Fe plate was removed the temperature of the substrate rose above 100 °C and the dc field had a

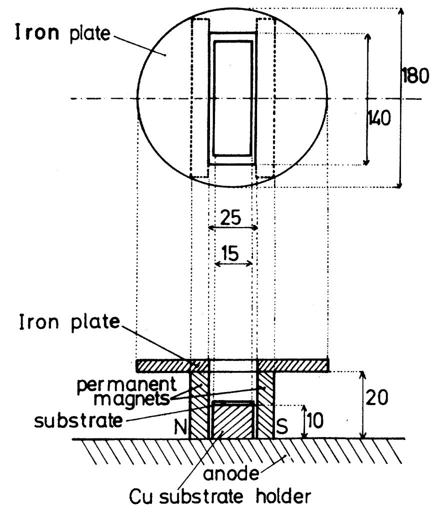

FIG. 1. Schematic diagram of the substrate holder (distances in mm).

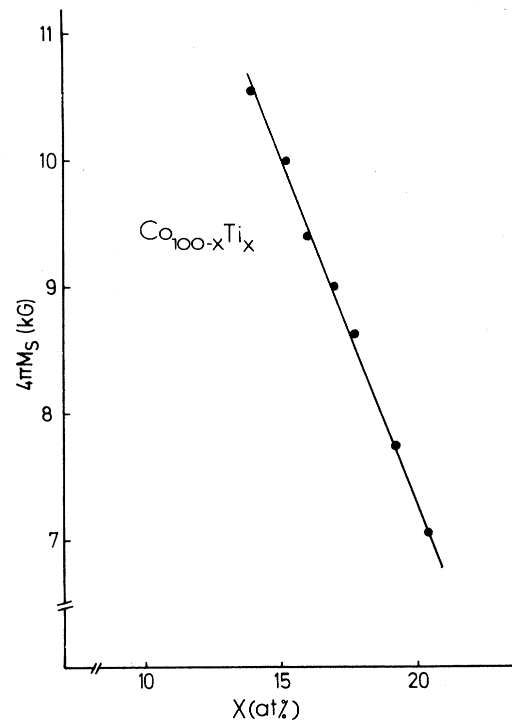

FIG. 2. Composition dependence of saturation magnetization at room temperature.

component out of the film plane, and we observed the formation of the perpendicular anisotropy.[20]

The films for magnetic measurements were deposited onto Corning 7059 glass substrates. The magnetic properties were investigated unless otherwise reported in the amorphous range which correspond to $x \geq 0.14$, on films of thickness (t) in the range of 0.05 to 0.4 μm.

III. FERROMAGNETIC RESONANCE MEASUREMENTS (FMR): DETERMINATION OF RELEVANT MAGNETIC PARAMETERS AND CHARACTERIZATION OF THE MAGNETIC HOMOGENEITY

The ferromagnetic resonance measurements were carried out at room temperature by a standard X-band spectrometer at $f = 9.8$ GHz. $4\pi M_s$, the g factor, and H_k were computed from the three resonance fields $H_\perp$, $H_\parallel^e$, and $H_\parallel^d$ using formulas (A5), (A8), and (A9) of the Appendix.

The perpendicular anisotropy field H_p was determined by comparing the value of $4\pi M_s$ obtained for films of same composition but deposited at various pressures. The measurements revealed that H_p is negligible except for some samples deposited at $P_{\mathrm{Ar}} = 15 \times 10^{-3}$ Torr. The values of $4\pi M_s$ obtained were independent of the deposition parameters within $\pm 3\%$ in the concentration range $0.14 \leq x \leq 0.22$. Figure 2 shows the variation of $4\pi M_s$ with Ti concentration at room temperature. The results are in agreement with those obtained in previous investigations.[23]

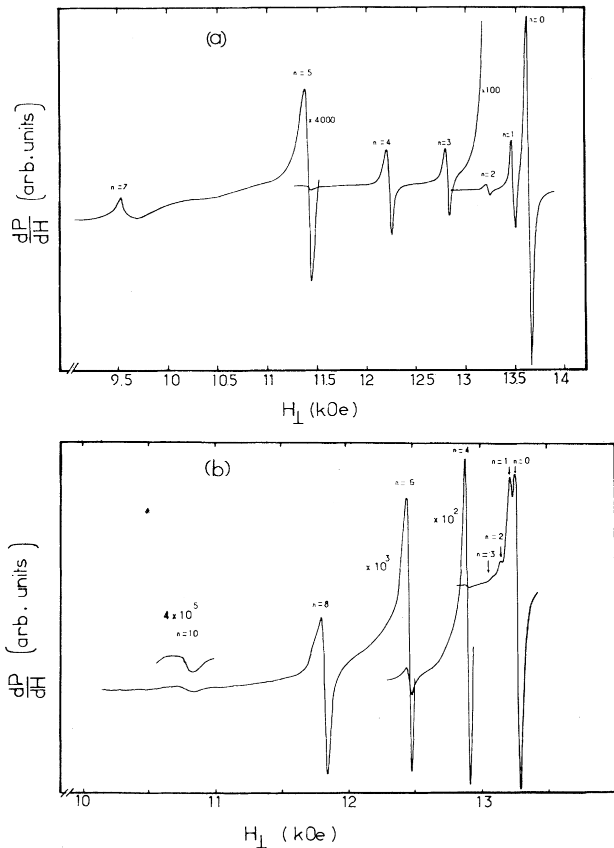

FIG. 3. Absorption derivative of the spin-wave resonance spectrum of typical samples for applied field perpendicular to the film plane: (a) $t = 0.18$ μm, (b) $t = 0.35$ μm.

FMR is also a suitable technique for the determination of the magnetic homogeneity of a soft ferromagnet prepared in thin-film form. In the present case for the whole concentration range and for all deposition parameters—except on some samples prepared at $P_{\mathrm{Ar}} = 15$ mTorr—we obtained a simple resonance spectrum. For $H_\perp$ the spectra are composed of a main mode followed by a series of weakly excited standing spin-wave (SSW) modes. In the parallel orientation only the main mode could be detected. These results show that the films are formed of a single magnetic phase, and no sublayers with different magnetic properties could be detected.

Typical resonance spectra on films of composition $Co_{86}Ti_{14}$ and respective thickness $t = 0.18$ μm and $t = 0.35$ μm are shown in Figs. 3(a) and 3(b). These spectra exhibit characteristics of a film with fairly small magnetic inhomogeneities and could be explained by the volume inhomogeneity model.[24]

For $H_\perp$, all the modes—except the main mode—follow fairly closely the classical quadratic dispersion relation

$$H_n = \frac{\omega}{\gamma} + \langle 4\pi M_s \rangle - D\frac{\pi^2}{d^2}n^2 ,$$

where n is an integer.[24] The inhomogeneity of the internal field along the film thickness could be estimated from $\delta H' = (4\pi M_s)_{\max} - \langle 4\pi M_s \rangle = H_0' - H_0$, where H_0' is the value given by the dispersion law extrapolated to $n = 0$ and H_0 the experimental resonance field corresponding to the main mode. On all samples investigated $\delta H'$ was in the range 50 Oe $< \delta H' <$ 150 Oe. No systematic correlation was found between $\delta H'$, the magnitude of H_k, and/or the deposition parameters.

The variation of the intensities I_n of the various spin-wave modes is also typical of a thin film with small magnetic inhomogeneities. In thinner layers ($t \leq 0.2$ μm) modes with both parities were usually detected, the intensity of the odd modes being stronger than that of the even ones. On thicker films ($t \geq 0.25$ μm) the odd modes were generally fairly weakly excited. These results and the fact that I_1/I_0 and I_2/I_0 decrease with increasing film thickness are in favor of the hypothesis that the magnetic homogeneity along the film thickness improves slightly with increasing film thickness. Figure 4(a) shows the variation of I_n/I_0 as a function of mode number for a film of thickness 0.35 μm. The variation of I_n/I_0 is close to $1/n^4$ as predicted for small magnetic inhomogeneities. Figure 4(b) shows the variation of the linewidth ΔH_n corresponding to the various spin-wave modes. ΔH_n increases with n, the increasing being particularly marked for the highest-order modes. It is believed that this result is related to a slight fluctuation in the film thickness. A change Δt in the thickness across the plane of the film broadens the line by[25]

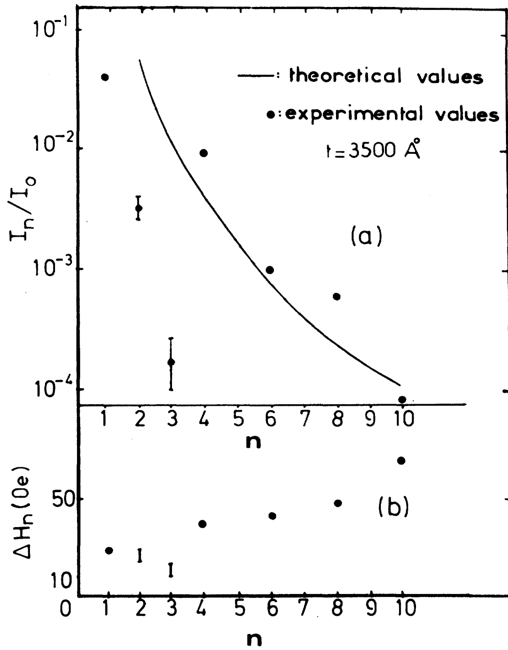

FIG. 4. (a) Dependence of the intensity of the various spin-wave modes as compared to $I_n \propto 1/n^4$. (b) Dependence of the linewidth ΔH_n on mode number n; $t = 0.35$ μm.

$$\Delta H_n = \Delta H_n^0 + D \frac{n^2\pi^2}{t^2} \frac{2\Delta t}{t} . \quad (1)$$

In the perpendicular configuration the derivative linewidth corresponding to the uniform mode is $\Delta H_\perp = (45 \pm 5)$ Oe and independent of film thickness in the thickness range investigated, i.e., for $0.05 \le t \le 0.4$ μm. The value of the linewidth $\Delta H_\parallel$ in parallel configuration is closed to $\Delta H_\perp$, with $|\Delta H_\perp - \Delta H_\parallel| / \Delta H_\perp < 0.1$. These results can be easily understood if we consider the various contributions to $\Delta H_\perp$ given by $\Delta H_\perp = \Delta H_0 + \Delta H_{ed} + \Delta H_{def}$. ΔH_0 is the intrinsic damping and is generally related to spin-orbit interactions. ΔH_{ed} is related to the contribution of the exchange conductivity mechanism to the damping. The resistivity of amorphous $Co_{86}Ti_{14}$ is typically of the order of $\rho = (130 \pm 10)$ $\mu\Omega$ cm.[13] The corresponding rf skin depth is $\delta = c/\sqrt{2\omega\delta} = 5.79$ μm. As this value is an order of magnitude larger than the thickness range investigated, the eddy current contribution to the relaxation process for the thickness range investigated is negligible. ΔH_{def} is the linewidth related to the various defects and is at the origin of a two-magnon relaxation process. ΔH_{def} arises from inhomogeneities of local anisotropy fields and/or from fluctuation of the local exchange interactions. The overall results are in favor of the hypothesis that the contribution of the defects to $\Delta H_\perp$ is small so the as-observed value of $\Delta H_\perp = (45 \pm 5)$ Oe is essentially a measure of the intrinsic magnetic damping.

Figure 5 shows the value of the exchange constant D. The results differ by less than 20% from that obtained previously, the main uncertainties arising from thickness measurements.

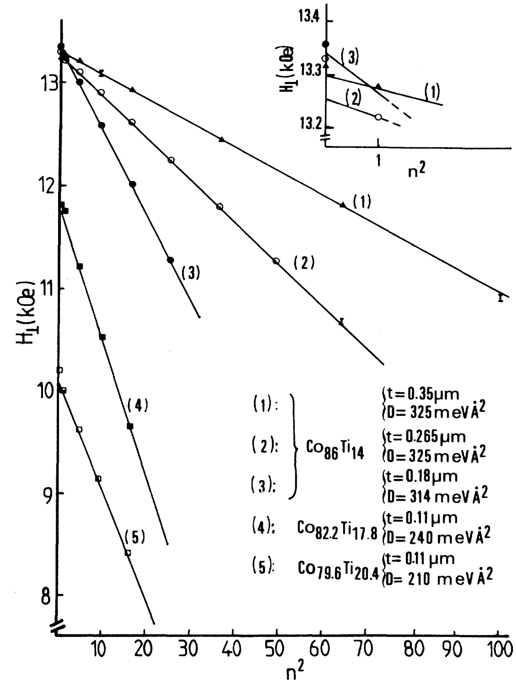

FIG. 5. Spin-wave resonance field as a function of mode number for perpendicular orientation. (1)–(3): films of same composition and various thickness, (4) and (5): films of various concentration. In the inset an enlarged version of the deviation of the low-order modes is shown.

IV. CHARACTERISTICS OF THE *B-H* LOOP

A systematic study of the in-plane *B-H* loop performed by the use of a classical *B-H* loop tracer working at $f = 50$ Hz revealed the following general characteristics. Along the easy axis the hysteresis loops are rectangular for the whole concentration range and the various deposition parameters used. Along the hard axis the loops are characterized by an extremely well-defined in-plane uniaxial anisotropy field. The opening of the loop was generally not detectable. H_k was also studied by in-plane angular resonance measurements. A set of experimental resonance fields and the corresponding computed curves obtained using formulas (A6) and (A7) are shown in Fig. 6 for some typical samples. Figure 7 shows a comparison of the values of H_k obtained from *B-H* loop and FMR measurements. The values of H_k agree within $\pm 5\%$. From these experiments one can conclude that the dispersion of H_k is fairly low.

Transverse susceptibility measurements confirmed these results.[26] The angular dispersion of H_k was independent of its magnitude and typically in the range of 0.25 to 0.5°.

V. INDUCED UNIAXIAL ANISOTROPY K_u

The variation of K_u was studied systematically as a function of the pressure of the sputter gas P_{Ar}, and the rf

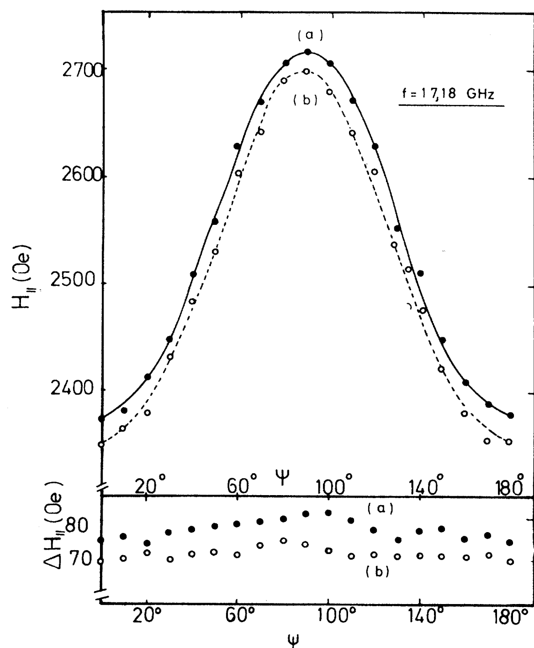

FIG. 6. In-plane variation of the resonance field and corresponding $\Delta H_{\parallel}$ as determined by in-plane FMR measurements for two layers (a) and (b), and — — —; computed curves, ●; and ○, experiments.

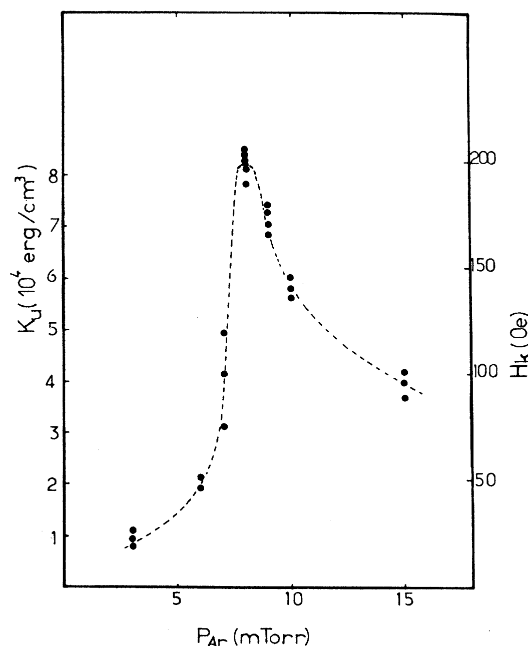

FIG. 8. Variation of K_u as a function of P_{Ar} in a-$Co_{86}Ti_{14}$.

input power W_{rf}. The experiments revealed that the value of K_u is nearly independent of W_{rf} and is essentially related to P_{Ar}. Figure 8 shows the variations of K_u with argon pressure for $Co_{86}Ti_{14}$.[19] With increasing P_{Ar} one observes a bell-shaped variation of K_u with a fairly well-defined maximum $(K_u)_{max}$ for $P_{Ar}=8$ mTorr. K_u decreases more gradually for higher P_{Ar}. The value of K_u was a minimum $(K_u)_{min}$ for the lowest P_{Ar} used, i.e., $P_{Ar}=3$ mTorr.

The trend of the variation of $K_u(x)$ with P_{Ar} is the same for the whole concentration range studied. In particular $[K_u(x)]_{max}$ and $[K_u(x)]_{min}$ always occur at the same pressure. Figure 9 shows the variation of $K_u(x)$ as a function of Ti content x for the three different charac-

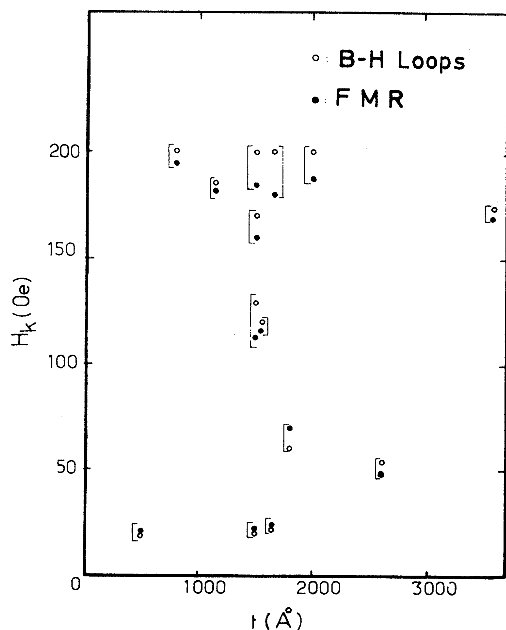

FIG. 7. Value of H_k as deduced from B-H loop (●) and from in-plane FMR measurements (○).

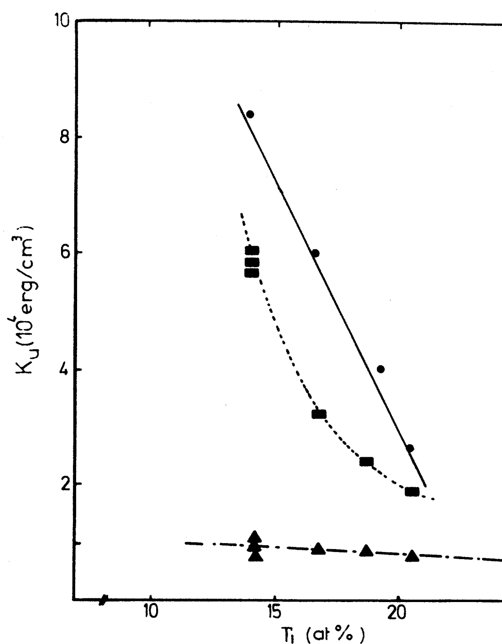

FIG. 9. Concentration dependence of K_u as a function of Ti content for three different values of P_{Ar}, (▲), 3×10^{-3} Torr; (●), 8×10^{-3} Torr; and (■), 15×10^{-3} Torr.

teristic values of P_{Ar}.

We explained the overall results by a model based upon the local structure of $Co_{1-x}Ti_x$ amorphous films.[19] The structure of $Co_{1-x}Ti_x$ is formed of a random continuous matrix of clusters with trigonal (hcp-like), octahedral (fcc-like), and icosahedral symmetries. K_u can originate from pseudodipolar and/or structural anisotropy. The structural anisotropy is essentially related to the local anisotropy K_1 corresponding to Co atoms in trigonal clusters as the anisotropy due to Co atoms located in octahedral or icosahedral clusters can be considered to be fairly low. In accordance with the thermomagnetic hysteresis observed on CoNbB (Ref. 27) amorphous alloys the lower and higher anisotropy state is developed at $T > T_{cr}$ and $T < T_{cr}$, respectively, with a phase transformation around the critical temperature T_{cr} requiring a well-defined activation energy Q.

The number and orientation of various clusters vary with P_{Ar}, as P_{Ar} determines the energy of the particles E^F so their effective temperatures as they arrive at the substrate. E^F can be computed by considering the energy loss for sputtered atoms as they travel through the sputtering gas using the formula[28]

$$E^F=(E_0-k_BT_G)\exp\left[n\ln\frac{E_f}{E_i}\right]+k_BT_G\ , \tag{2}$$

where E_0 is the energy of the particle as it leaves the target, T_G the sputtering gas temperature, E_f/E_i the ratio of energies before and after a collision, and n the number of collisions of the sputtered atoms with Ar, determined by

$$n=\frac{lP_{Ar}S}{k_BT_G}\ , \tag{3}$$

where l is the target-substrate distance and S the collision cross section evaluated from the free particle atomic radii.

The average loss per collision is given by

$$\ln\frac{E_f}{E_i}=1-\frac{(M-1)^2}{2M}\ln\left|\frac{M+1}{M-1}\right|\ , \tag{4}$$

where M is the ratio of the atomic mass of the sputtered atoms to that of the Ar atoms. The as-computed E^F corresponding to Co and Ti particles versus P_{Ar} is reported on Fig. 10 where we used $E_0(\text{Co})=3.25$ eV, $E_0(\text{Ti})=4.05$ eV,[29] $S(\text{Co})=21.56\times10^{-20}\text{m}^2$, $S(\text{Ti})=25.3410^{-20}\text{m}^2$, and $T_G=400$ K. The deposit is instantaneously quenched down to room temperature, so that E^F can be considered as the activation energy Q available in the solid state. Let us consider E^F for three characteristic values of P_{Ar}, i.e., $P_{Ar}=3$, 8, and 15 mTorr. When $P_{Ar}=3$ mTorr the $E^F_{Co}=1.17$ eV and $E^F_{Ti}=1.09$ eV. As a result the value of Q is fairly high so that the sample is built up essentially of icosahedral and octahedral clusters. For $P_{Ar}=15$ mTorr, $E^F_{Co}=0.053$ eV and $E^F_{Ti}=0.04$ eV. Now the sputtered atoms are practically thermalized to the temperature of the plasma $T=400$ K. The effective temperature of the particles is low, a condition corresponding to the development of a significant number of trigonal clusters, and consequently, for this pressure the value of K_u is much higher than for 3 mTorr. However, Q is out of the range for which a significant phase transformation occurs, so that the probability of trigonal-like clusters to be oriented along the applied field is small. When $P_{Ar}=8$ mTorr, conditions for which K_u is maximum, $E^F_{Co}=0.24$ eV and $E^F_{Ti}=0.15$ eV. These values are close to the activation energy $Q=0.15$ eV determined by Corb *et al.*[27] for which the phase transformation is the largest. As the sample is cooled down, some of the icosahedral clusters are transformed to trigonal ones. During this transformation the trigonal clusters will be oriented along the applied field in order to minimize the total energy acting on the film. The decreases of $(K_u)_{max}$ with increasing Ti concentration is simply related to a more disordered local structure.

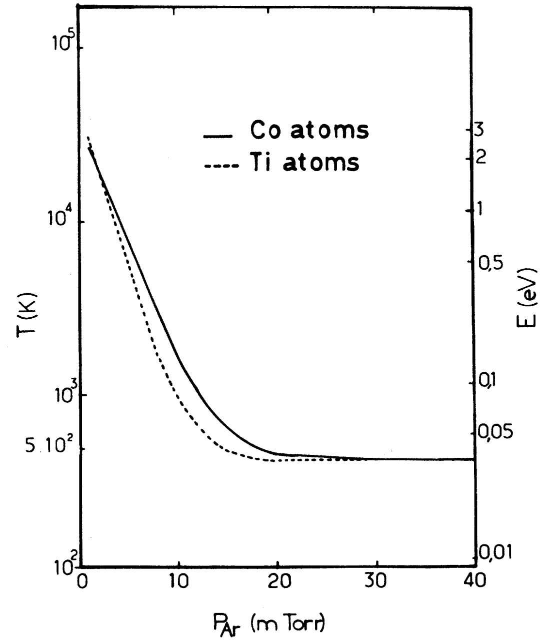

FIG. 10. Calculated energies of Co and Ti particles as a function of P_{Ar}. The computation was performed for $l=75$ mm with constants given in the text.

It is believed that the proposed mechanism is analogous to the formation of induced anisotropy in crystalline Co and CoNi, when these alloys are cooled in a strong external magnetic field. [30] The induced anisotropy is related to the fcc-hcp transformation: Its high value was attributed by Graham[30] to the formation of a crystallographic texture in the hcp phase, where the crystallographic direction corresponding to the easy magnetic axis tends to be oriented parallel to the applied field.

VI. EXPERIMENTAL DISCRIMINATION BETWEEN STRUCTURE-RELATED AND PSEUDODIPOLAR ANISOTROPY: ANNEALING AND ION MIXING

If the field-induced anisotropy is related to the pseudodipolar anisotropy via directional ordering of the

transition-metal atoms, it is a reversible phenomenon. The easy axis can be reoriented along various directions by annealing in a magnetic field, and the magnitude of K_u saturates after a certain length of annealing. If the field-induced anisotropy is related to the local structure, annealing should not change the value of K_u unless the local structure is changed or crystallization occurs.

We studied the variation of K_u in a-$Co_{86}Ti_{14}$ films as a function of isothermal annealing using the rotating field annealing technique.[31] The annealing was performed in the temperature range 150–350 °C and for a length of 1 h and gave the following results. On samples deposited at $P_{Ar}=3\times10^{-3}$ Torr, H_k is almost suppressed. On samples deposited in the pressure range $3\times10^{-3}<P_{Ar}<8\times10^{-3}$ Torr, a part of the anisotropy field, typically $H_k\approx20$ Oe, could be suppressed. On samples deposited at $P_{Ar}>8\times10^{-3}$ Torr, H_k is unchanged. These results can be explained as follows. For 3×10^{-3} Torr, K_u is essentially due to a pseudodipolar anisotropy, the structure-related anisotropy being negligible. For $P_{Ar}>8\times10^{-3}$ Torr, K_u is mainly due to the local anisotropy in agreement with the structural model proposed. For the intermediate pressure range K_u is the sum of structure-related and pseudodipolar anisotropy.

Rare-gas implantation enabled also the two types of anisotropy to be distinguished.[32] In $Co_{86}Ti_{14}$ thin films implanted at 10^{16} Xe^+/cm^2, K_u was completely suppressed irrespective of its initial value. These films were subsequently annealed in a magnetic field of 1600 Oe at 250 to 300 °C during 1 to 20 h. In all samples K_u appeared to saturate at 7.10^3 to 8.10^3 erg/cm^3 showing this to be the maximum amount of the pseudodipolar K_u.

The concentration dependence of K_u is shown in Fig. 9. K_u decreases with increasing Ti concentration as reported for films obtained at the three different characteristic pressures. We explain this result as follows: On samples deposited at 8 and 15×10^{-3} Torr, K_u is due to the local anisotropy. A more disordered local structure is formed with increasing Ti concentration. As a result the trigonal clusters lower their bond orientational order and the corresponding value of K_1 decreases.

On samples deposited at 3×10^{-3} Torr, K_u is due to a pseudodipolar interaction via a chemical short-range order, due to the existence of a monoatomic directional order, or a directional pair ordering of a single magnetic species in an inhomogeneous environment. According to the theory K_u is given by

$$K_u=A\frac{W(T)W(T_A)}{15\ \mathrm{kT}_A}f(x)\ , \tag{5}$$

where $f(x)=x$ for a monoatomic model and $f(x)=zNx^2(1-x)^2$ for a pair ordering model,[34] where it is assumed that only Co-Co interactions contribute to K_u. In this expression W is the pseudodipolar interaction, N the total number of atoms, z the number of nearest neighbors, T_A is the annealing, and T the measuring temperature. If $W(T)$ and $W(T_A)$ are concentration independent K_u should increase with increasing x following both models, which is contrary to the experimental results. However, the Curie temperature of $Co_{1-x}Ti_x$ depends strongly upon Ti concentration[23] so the concentration dependence of dipole-dipole interaction has to be taken into account. Generally it is assumed that $W(T)$ is proportional to $M_s^2(T)$ (Ref. 11) so Eq. (5) becomes

$$K_u=\frac{AW^2(0)}{15\ kT_A}\left[\frac{M_s(T)}{M_s(0)}\right]^2\left[\frac{M_s(T_A)}{M_s(0)}\right]^2 f(x)\ . \tag{6}$$

The value of $M_s(T_A)$ for the various alloys is not known so when K_u is related to a directional short-range order it is not possible to say if the existing theory permit to explain the concentration dependence of K_u.

VII. COERCIVE FIELD

Figure 11 shows the variation of H_c as a function of Ti concentration in the deposit. H_c decreases rapidly in the concentration range $0.07<x<0.13$ and becomes almost independent of concentration for a given set of deposition parameters when $x>0.14$. This result is simply related to the transition from a microcrystalline to the amorphous state. In the microcrystalline state the main contributions to H_c arise from the randomly distributed magnetocrystalline anisotropy and domain-wall pinning at grain boundaries. The number and the size of microcrystals decrease continuously with increasing Ti content[32] which explains the observed variation of H_c.

In the amorphous state ($x\geq14$) we observed some slight but significant variation of H_c as a function of the deposition parameters P_{Ar} and W_{rf}. The results reported in Fig. 12 were obtained on thin films of composition $Co_{86}Ti_{14}$ but the overall trends for the whole concentration range were similar. The dependence of H_c upon P_{Ar} is shown for $W_{rf}=200$ W. For the pressure range $8\leq P_{Ar}\leq15$ mTorr, H_c increases with increasing P_{Ar}. This result is probably related to the change of the local structure with P_{Ar}. When $P_{Ar}>8$ mTorr the number of

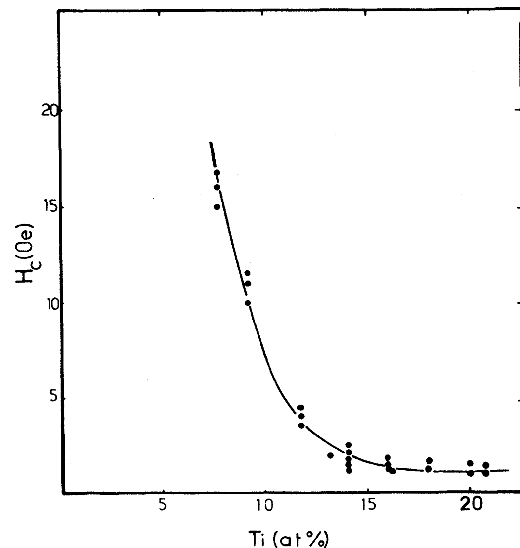

FIG. 11. Variation of the coercive field H_c as a function of Ti concentration.

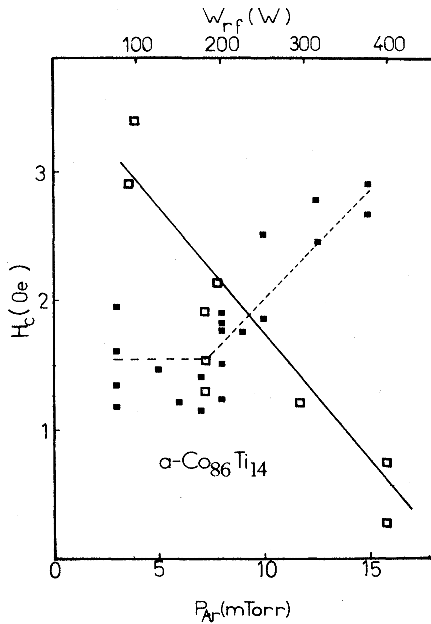

FIG. 12. Variation of H_c as a function of deposition parameters ■, H_c as a function of P_{Ar} for $W_{rf}=200$ W; □, H_c as a function of W_{rf} for $P_{Ar}=3$ mTorr.

randomly distributed trigonal clusters increases and the contribution of the related local anisotropy field to H_c could explain the results. The dependence of H_c upon W_{rf} was particularly marked in films deposited at low pressure ($P_{Ar}=3\times10^{-3}$ Torr), and H_c decreased continuously with increasing W_{rf}. W_{rf} determines the deposition rate and a possible interpretation of the results is that for higher deposition rates the number of nonmagnetic inclusions is lower.

VIII. CONCLUSIONS

We reported the overall magnetic properties of a-$Co_{1-x}Ti_x$ ferromagnetic thin films for the concentration range $0.14\leq x\leq0.22$. The films were prepared by rf sputtering and during the deposition process a magnetic field was applied parallel to the substrate surface. In order to avoid the formation of an anisotropy perpendicular to the film plane it is necessary to use a substrate holder which possesses a particular geometrical configuration. For the whole range of deposition parameters investigated, the films exhibit soft ferromagnetic properties. They have highly uniform magnetic properties along their thickness for the deposition parameter used as revealed by FMR measurements. The value and the physical origin of K_u for a given concentration depend essentially on the pressure of the sputtering gas P_{Ar}. At low P_{Ar} ($P_{Ar}=3\times10^{-3}$ Torr), K_u is related to a pseudodipolar

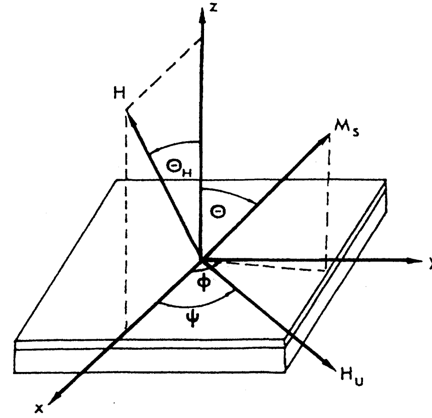

FIG. 13. Coordinates system showing the various angles used in the computation.

short-range ordering, while at high P_{Ar} ($P_{Ar}\geq8\times10^{-3}$ Torr) the high value of K_u is due to the local anisotropy of Co atoms located in trigonal clusters. For the intermediate range of P_{Ar}, K_u appears to be the sum of these two types of anisotropy. The physical origin of K_u could be determined experimentally by magnetic annealing. The value of the coercive field H_c is fairly small and varies slightly with W_{rf} and P_{Ar}. This variation is believed to be due to the evolution of local defects and local anisotropy, respectively.

APPENDIX: EXPRESSION FOR FERROMAGNETIC RESONANCE FOR A THIN FILM WITH AN IN-PLANE UNIAXIAL ANISOTROPY

Consider a thin film with an in-plane uniaxial field $H_k=2K_u/M_s$. The coordinate system is shown in Fig. 13. The external field **H** lies in the $x0z$ plane and is inclined at an angle ϑ_H to the z axis. ϑ and Φ are the customary angles defining the direction of the magnetization $\mathbf{M}_s$ and ψ is the angle between the easy axis of the anisotropy field and $0x$. The resonance conditions can be obtained from the free energy per unit volume which is given by

$$E=-M_sH(\sin\theta\cos\Phi\sin\theta_H+\cos\theta\cos\theta_H)$$
$$+2\pi M_s^2\cos^2\theta-K_u\sin^2\theta\cos^2(\Phi-\Psi)\ . \qquad \text{(A1)}$$

In the above equation the first term is the Zeeman energy, the second term the demagnetizing energy, and the third term the anisotropy energy. The resonance formula for an arbitrary orientation ϑ_H of the applied field follows from the equation

$$\left[\frac{\omega}{\gamma}\right]^2=\{H(\cos\theta\cos\theta_H+\sin\theta\sin\theta_H\cos\Phi)+H_k\cos2(\Phi-\Psi)-[4\pi M_s+H_k\cos^2(\Phi-\Psi)]\cos2\theta\}$$
$$\times\{H(\cos\theta\cos\theta_H+\sin\theta\sin\theta_H\cos\Phi)-\cos2\theta[4\pi M_s+H_k\cos^2(\Phi-\Psi)]\}-[\tfrac{1}{2}H_k\cos\theta\sin2(\Psi-\Phi)]^2 \qquad \text{(A2)}$$

and the corresponding equilibrium conditions are given by

$$H \sin\Phi \sin\theta_H = \frac{H_k}{2} \sin\theta \sin 2(\Psi - \Phi) , \quad \text{(A3)}$$

$$H(\sin\theta \cos\theta_H - \cos\theta \sin\theta_H \cos\Phi) = 2\pi M_s \sin 2\theta + \frac{H_k}{2} \sin 2\theta \cos^2(\Phi - \Psi) . \quad \text{(A4)}$$

Let us consider Eqs. (A2)–(A4) for some particular orientation of the applied field. When the applied field is perpendicular ($H_\perp$) to the film plane $\theta_H = \theta = \Phi = 0$ and Eqs. (A2)–(A4) reduce to

$$\left[\frac{\omega}{\gamma}\right]^2 = (H_\perp - 4\pi M_s)(H_\perp - 4\pi M_s - H_k) . \quad \text{(A5)}$$

When H lies in the plane of the thin film $\theta_H = \theta = \pi/2$. The resonance condition is given by

$$\left[\frac{\omega}{\gamma}\right]^2 = [H \cos\Phi + H_k \cos 2(\Phi - \Psi)] \times [H \cos\Phi + 4\pi M_s + H_k \cos^2(\Phi - \Psi)] \quad \text{(A6)}$$

and the equilibrium relation by

$$H \sin\Phi = \frac{H_k}{2} \sin 2(\Psi - \Phi) . \quad \text{(A7)}$$

These formulas are further reduced when the applied field is parallel $H_\parallel^e$ ($\psi = 0$) or perpendicular $H_\parallel^d$ ($\psi = \pi/2$) to the in-plane easy axis. For these two configurations M_s and H are parallel ($\Phi = 0$) and the resonance conditions are, respectively,

$$\left[\frac{\omega}{\gamma}\right]^2 = (H_\parallel^e + H_k)(H_\parallel^e + H_k + 4\pi M_s) , \quad \text{(A8)}$$

$$\left[\frac{\omega}{\gamma}\right]^2 = (H_\parallel^d - H_k)(H_\parallel^d + 4\pi M_s) . \quad \text{(A9)}$$

From the three resonance fields $H_\perp$, $H_\parallel^e$, and $H_\parallel^d$, one can compute $4\pi M_s$, H_k, and the gyromagnetic ratio γ. When the condition $H_k \ll 4\pi M_s$ is satisfied (which is generally the case), the expression

$$H_k \approx \frac{H_\parallel^d - H_\parallel^e}{2}$$

constitutes a fairly good approximation for H_k.

[1]C. H. Wilts and F. B. Humphrey, J. Appl. Phys. **39**, 1191 (1968).

[2]See, for example, H. Fujimori, *Magnetic Anisotropy in Amorphous Metallic Alloys* (Butterworths, London, 1982).

[3]B. S. Berry and W. C. Prichet, Phys. Rev. Lett. **34**, 1022 (1975).

[4]T. Miyazaki and M. Takashashi, Jpn. J. Appl. Phys. **10**, 1755 (1978).

[5]F. E. Luborsky and J. L. Walter, IEEE Trans. Magn. **MAG-13**, 953 (1977).

[6]H. Kronmüller, Phys. Status Solidi B **118**, 661 (1981).

[7]T. Miyazaki, M. Takahashi, and H. Hisatake, J. Appl. Phys. **57**, 3575 (1985).

[8]W. Chambron and A. Chamberod, Solid State Commun. **35**, 61 (1980).

[9]L. Neel, J. Phys. Rad. **15**, 225 (1954).

[10]S. Taniguchi, Sci. Rep. Res. Inst. Tohoku Univ., Ser. A: **7**, 269 (1955).

[11]J. C. Slonczewski, in *Magnetism*, edited by G. T. Rado and H. Suhl (Academic, New York, 1963), Vol. 1, p. 205.

[12]T. Miyazaki and M. Takashashi, J. Magn. Magn. Mater. **42**, 29 (1984).

[13]J. A. Aboaf and E. Klokholm, J. Appl. Phys. **52**, 1184 (1981).

[14]Y. Shimada and H. Kojima, J. Appl. Phys. **53**, 3156 (1981).

[15]N. S. Kazama, H. Fujimori, and K. Hirose, IEEE Trans. Magn. **MAG-18**, 1185 (1983).

[16]J. I. Guzman and M. H. Kryder, J. Appl. Phys. **61**, 3240 (1987).

[17]T. Jagielinski, J. Appl. Phys. **61**, 3237 (1987).

[18]G. Suran and K. Ounadjela, J. Magn. Magn. Mater. **54-57**, 2137 (1985).

[19]G. Suran, K. Ounadjela, and F. Machizaud, Phys. Rev. Lett. **57**, 3109 (1986).

[20]G. Suran, K. Ounadjela, and F. Machizaud, J. Appl. Phys. **61**, 3658 (1987).

[21]G. Suran, K. Ounadjela, J. Sztern, and C. Sella, J. Appl. Phys. **55**, 1757 (1984).

[22]K. Ounadjela, G. Suran, and J. Sztern, Thin Solid Films **151**, 397 (1987).

[23]G. Suran, J. Sztern, J. A. Aboaf, and T. R. McGuire, IEEE Trans. Magn. **MAG-17**, 3065 (1981).

[24]F. Hoffmann, Solid State Commun. **9**, 295 (1971).

[25]G. C. Bailey, J. Appl. Phys. **41**, 5232 (1970).

[26]K. Le Dang, P. Veillet, G. Suran, and K. Ounadjela, J. Appl. Phys. **62**, 3328 (1987).

[27]B. W. Corb, R. C. O'Handley, J. Megusar, and N. J. Grant, Phys. Rev. Lett. **51**, 1386 (1983).

[28]F. J. Cadieu and N. Chencinski, IEEE Trans. Magn. **MAG-11**, 227 (1975).

[29]J. Bessot, Soc. Fr. Vide **1**, 169 (1985).

[30]C. D. Graham, Jr., J. Phys. Soc. Jpn. **17-B1**, 321 (1962).

[31]G. Suran and F. Materne, Solid State Commun. **68**, 21 (1988).

[32]G. Suran and P. Gerard, IEEE Trans. Magn. (to be published).

[33]Y. Machata, T. Yamimori, M. Hattori, S. Tsunashima, and S. Uchiyama, Fifth International Conference on Rapidly Quenched Metals 239, 1984 (unpublished).

[34]K. Ounadjela, Ph.D. thesis Université de Paris VII, 1986.